REGULAR ARTICLE

blood advances

Elevated CDKN1A (P21) mediates β-thalassemia erythroid apoptosis, but its loss does not improve β-thalassemic erythropoiesis

Raymond Liang,[1,2,*] Miao Lin,[1,*] Vijay Menon,[1] Jiajing Qiu,[1] Anagha Menon,[1,2] Laura Breda,[3] Tasleem Arif,[1] Stefano Rivella,[3] and Saghi Ghaffari[1,2,4-6]

[1]Department of Cell, Developmental & Regenerative Biology and [2]Developmental and Stem Cell Biology Multidisciplinary Training, Graduate School of Biomedical Sciences, Icahn School of Medicine at Mount Sinai, New York, NY; [3]Division of Hematology, Children's Hospital of Philadelphia, University of Pennsylvania, Philadelphia, PA; and [4]Department of Oncological Sciences, [5]Black Family Stem Cell Institute, and [6]Tisch Cancer Institute, Icahn School of Medicine at Mount Sinai, New York, NY

Key Points

- Elevated P21 or FOXO3 mediates β-thalassemia erythroid cell apoptosis.
- Loss of FOXO3 or P21 reduces β-thalassemia erythroid cell apoptosis but loss of neither improves β-thalassemic ineffective erythropoiesis.

β-thalassemias are common hemoglobinopathies due to mutations in the β-globin gene that lead to hemolytic anemias. Premature death of β-thalassemic erythroid precursors results in ineffective erythroid maturation, increased production of erythropoietin (EPO), expansion of erythroid progenitor compartment, extramedullary erythropoiesis, and splenomegaly. However, the molecular mechanism of erythroid apoptosis in β-thalassemia is not well understood. Using a mouse model of β-thalassemia ($Hbb^{th3/+}$), we show that dysregulated expression of the FOXO3 transcription factor is implicated in β-thalassemia erythroid apoptosis. In $Foxo3^{-/-}/Hbb^{th3/+}$ mice, erythroid apoptosis is significantly reduced, whereas erythroid cell maturation, and red blood cell and hemoglobin production are substantially improved even with elevated reactive oxygen species in double-mutant erythroblasts. However, persistence of elevated reticulocytes and splenomegaly suggests that ineffective erythropoiesis is not resolved in $Foxo3^{-/-}/Hbb^{th3/+}$. We found the cell cycle inhibitor *Cdkn1a* (cyclin-dependent kinase inhibitor *p21*), a FOXO3 target gene, is markedly upregulated in both mouse and patient–derived β-thalassemic erythroid precursors. Double-mutant $p21/Hbb^{th3/+}$ mice exhibited embryonic lethality with only a fraction of mice surviving to weaning. Notably, studies in adult mice displayed greatly reduced apoptosis and circulating Epo in erythroid compartments of surviving $p21^{-/-}/Hbb^{th3/+}$ mice relative to $Hbb^{th3/+}$ mice, whereas ineffective erythroid cell maturation, extramedullary erythropoiesis, and splenomegaly were not modified. These combined results suggest that mechanisms that control β-thalassemic erythroid cell survival and differentiation are uncoupled from ineffective erythropoiesis and involve a molecular network including FOXO3 and P21. Overall, these studies provide a new framework for investigating ineffective erythropoiesis in β-thalassemia.

Introduction

β-thalassemias are 1 of the most common hemoglobinopathies globally, caused by >200 mutations in the β-globin gene. Patients experience variable degrees of anemia associated with a broad range of clinical manifestations.[1-3] Patients with β-thalassemia may be affected by severe anemia, requiring

Submitted 22 March 2022; accepted 24 August 2023; prepublished online on *Blood Advances* First Edition 6 September 2023. https://doi.org/10.1182/bloodadvances.2022007655.

*R.L. and M.L. contributed equally to the work.

The authors will make all detailed protocols available through request to the corresponding author, Saghi Ghaffari (saghi.ghaffari@mssm.edu).

The full-text version of this article contains a data supplement.

chronic blood transfusions for survival (β-thalassemia major), or milder clinical anemia requiring only sporadic transfusions (β-thalassemia intermedia), whereas patients with minor thalassemia are asymptomatic.[1-3]

Mutations in the β-globin gene lead to the absence or reduced β-globin synthesis. Decreased β-globin synthesis causes an imbalance in protein levels of α vs β chain, which disrupts production of functional adult $\alpha_2\beta_2$ hemoglobin A, a pathological mechanism that is most evident in homozygote β-thalassemia mutations. The accumulation of excessive unpaired α-globin chains in erythroblasts triggers redox-mediated reactions, leading to the generation of toxic aggregates that precipitate into red blood cell (RBC) precursors. In turn, the accumulation of α-globin aggregates result in premature death, ineffective erythroid maturation, and hemolytic anemia. Anemia induced by β-thalassemia further triggers the release of erythropoietin (EPO), which leads to the expansion of EPO–sensitive erythroid progenitors, leading to extramedullary erythropoiesis and splenomegaly. The increased apoptosis of late maturing erythroblasts is known as an aggravating factor in sustaining anemia despite enhanced erythropoiesis in patients with β-thalassemia,[4-6] which results in further expansion of extramedullary hematopoiesis. The clinical aspects of β-thalassemia are orchestrated in response to stress and elevated reactive oxygen species (ROS) in erythroid cells.[7-11] However, the source and regulation of elevated ROS levels remains debated and whether ROS are implicated in inducing apoptosis in β-thalassemia erythroid cells is unclear.[12] Importantly, the molecular underpinning of the enhanced apoptosis in β-thalassemia remains poorly understood.[4-6,12-16]

In the erythroid compartment, the transcription factor FOXO3 coordinates cell maturation and redox state.[17-21] FOXO3 is required for homeostatic erythropoiesis through regulation of a genetic program that promotes terminal erythroid maturation and enucleation.[14,17] These diverse functions are accomplished through transcriptional activation by FOXO3 of an array of genes including apoptotic genes in addition to cell cycle, antioxidant, and autophagy genes, depending on the cellular context.[22-26] A gradual increase in FOXO3 expression, nuclear localization, and transcriptional activity during erythroid maturation balances ROS levels in early vs late erythroblasts.[17,27] In early erythroid precursors, FOXO3 regulates erythroid cell cycling and differentiation. In late erythroblasts, FOXO3 is critical to terminal erythroid maturation, coordinated mitochondrial removal, and enucleation.[17,21,27-29] FOXO3 regulation of antioxidant genes in erythroid precursor cells, maintains the half-life of RBCs.[17] FOXO3 loss in erythroid cells is balanced by the activation of TP53 with which FOXO3 shares many targets and functions.[17,30-32] The steady upregulation of FOXO3 with maturation of primary mouse erythroblasts is not associated with apoptosis.[17] However, whether FOXO3 regulates apoptosis during erythropoiesis in the context of β-thalassemia is unknown; because FOXO3 can promote opposing pathways depending on cellular state, including inhibiting cell cycle or promoting cell cycle exit, inducing apoptosis, or promoting survival and differentiation.[30,33-36] Although FOXO3 is a target of TP53,[37] both factors have cross talk and share many common targets.[31,38] The cyclin-dependent kinase inhibitor P21 (CDKN1A, CIP1, WAF1) is a known direct target of both FOXO3 and TP53[39,40] that represses cell cycle entry in erythroid cells[17,41,42] but its function in β-thalassemia erythroid cells is largely unknown.[43]

Here, we asked whether FOXO3 is implicated in defects of β-thalassemia RBC production and subsequent abnormalities. We provide evidence that FOXO3 is prematurely activated in the β-thalassemia erythroid compartment; TP53 follows a similar pattern. We further show, using genetic approaches, that loss of either FOXO3, or its known target P21, significantly reduces β-thalassemia erythroid cell apoptosis. However, although FOXO3 loss improves anemia, it does not reduce splenomegaly or reticulocytosis in β-thalassemic mice. Alternatively, loss of P21 does not improve β-thalassemia anemia, extramedullary erythropoiesis, splenomegaly, or overall ineffective erythropoiesis. Altogether, these intriguing results suggest that mechanisms that control anemia, erythroid apoptosis, and ineffective erythropoiesis may be uncoupled in β-thalassemia. Our findings also uncover an intricate network between P21 and FOXO3 that includes TP53 in controlling β-thalassemia erythroid apoptosis.

Materials and methods

Mice

All protocols were approved by the institutional animal care and use committee of Mount Sinai School of Medicine. *Foxo3*$^{+/-}$ mice have been described previously.[30] Wild-type (WT) mice were used as controls in all experiments. For the majority of the experiments, 8- to 16-week-old mice were used. The β-thalassemic mice used have been described previously.[44] The *Foxo3*$^{-/-}$/*Hbb*$^{th3/+}$ double-mutant mice were generated by crossing the *Foxo3*$^{-/-}$ with the *Hbb*$^{th3/+}$ mice. *P21*$^{-/-}$ mice (Jackson Laboratory) were crossed with *Hbb*$^{th3/+}$ mice. Birth frequency of *p21*$^{-/-}$/*Hbb*$^{th3/+}$ deviated significantly from Mendelian inheritance (χ^2 test, $P < .0001$), suggesting occurrence of prenatal lethality.

Cell isolation and fluorescence-activated cell sorting (FACS) staining

Bone marrow cells were isolated from WT, *Foxo3*$^{-/-}$, *p21*$^{-/-}$, *Hbb*$^{th3/+}$, *Foxo3*$^{-/-}$/*Hbb*$^{th3/}$, or *p21*$^{-/-}$/*Hbb*$^{th3/+}$ mice by flushing the tibia and femurs with ice cold Iscove Modified Dulbecco Medium (IMDM, Gibco, catalog no. 12440-053) + 2% fetal bovine serum (FBS). These were then filtered through a 70-μm cell strainer, washed with 2% FBS/phosphate-buffered saline (PBS) and stained with TER119-Fluorescein isothiocyanate (FITC; BD Biosciences, catalog no. 557915) or TER119-V450 (BD Biosciences, catalog no. 560504), CD44-Pacific Blue (PB; BD Biosciences, catalog no. 560451), or CD44-Phycoerythrin (PE; BD Biosciences, catalog no. 553134), and CD45-Allophycocyanin (APC; BD Biosciences, catalog no. 559864) at 1:100 dilution in 2% FBS/PBS, and incubated at room temperature for 10 minutes. Cells were washed and resuspended in IMDM + 2% FBS containing 4′,6-diamidino-2-phenylindole (DAPI; for viability testing; 1 μg/mL). For the analysis of mitochondrial network, cells were incubated with 100 nM Mitotracker Green probe (Invitrogen Molecular Probes, catalog no. M7514) for 20 minutes at 37°C, after staining with primary antibodies. Cytoflow acquisition was carried out on the BD LSRII and cell sorting was performed on a BD Influx (Flow Cytometry Facility-Icahn School of Medicine at Mount Sinai) instrument. All cytometry analysis and quantifications were carried out using the FlowJo 10 software (TreeStar).

Immunoblotting

TER119$^+$ cells isolated from WT, *Foxo3*$^{-/-}$, and the *Hbb*$^{th3/+}$ mice were boiled directly in Laemmli sample buffer at 95°C for 10 minutes and stored at −80 °C till further use. Electrophoresis was carried out and the gels were transferred onto a polyvinylidene fluoride (PVDF) Immobilon-P membrane (Millipore). Membranes were then blocked with 5% bovine serum albumin (BSA)/1 × PBS/0.1% Tween-20 solution. After 3 washes, the membranes were incubated with the respective primary antibodies overnight at 4°C in 1% BSA/1× PBS/0.1% Tween-20 solution. After further washes, the membranes were then incubated with the secondary antibodies for 1 hour at room temperature. The blots were then washed 3 times and developed using the ECL reagent (Pierce). CD34$^+$ cells were isolated from blood obtained from healthy controls and patients with β-thalassemia, lysates prepared as described earlier, and probed with anti-P21 antibody. The blots were then washed and developed using the enhanced chemiluminescence (ECL) reagent. Antibodies used against TP53 upregulated modulator of apoptosis (PUMA, or BCL2-binding component 3; Novus Biologicals, catalog no. NB100-56623SS), ACTB (Cell Signaling, catalog no. 4970S), and P21 (Cell Signaling, catalog no. 2947).

EPO measurement

Using heparin as an anticoagulant, plasma was collected from blood obtained from WT, *p21*$^{-/-}$, *Hbb*$^{th3/+}$, and *p21*$^{-/-}$/*Hbb*$^{th3/+}$ mice. It was then centrifuged for 20 minutes at 2000*g* within 30 minutes of collection. EPO was quantified using the mouse erythropoietin/EPO Quantikine enzyme-linked immunosorbent assay kit (R&D Systems, catalog no. MEP00B), per the manufacturer's instructions.

Hematological studies

Blood samples were obtained from WT, *Foxo3*$^{-/-}$, *Hbb*$^{th3/+}$, *p21*$^{-/-}$, *Foxo3*$^{-/-}$/*Hbb*$^{th3/+}$, and *p21*$^{-/-}$/*Hbb*$^{th3/+}$ mice, immediately after euthanization of the mice and collected in EDTA or heparin. Complete blood counts were measured at the Comparative Pathology laboratory at Mount Sinai using an Advia 120 analyzer.

Intracellular ROS measurements

TER119$^+$ cells were isolated from the bone marrow of indicated mice. These cells were washed with PBS and then resuspended in PBS supplemented with 2% fetal calf serum or FBS and 5μM CM-H2DCFDA (chloromethyl derivative of 2' ,7' -dichlorodihydrofluorescein diacetate [H_2DCFDA]) probe (Invitrogen Molecular Probes, catalog no. 1034012) and incubated in the dark for 20 minutes at 37°C under 5% CO_2. The oxidative conversion of CM-H2DCFDA to the fluorescent product was measured using flow cytometry, as previously described.[45,46]

Apoptosis assay using annexin V–propidium iodide (PI) or 7-aminoactinomycin D staining

Erythroblasts from the bone marrow or spleen were isolated from WT, *Foxo3*$^{-/-}$, *Hbb*$^{th3/+}$, *21*$^{-/-}$, *Foxo3*$^{-/-}$/*Hbb*$^{th3/+}$, and *p21*$^{-/-}$/*Hbb*$^{th3/+}$ mice, as previously described.[45,46] Erythroblasts of indicated stages, stained with TER119 and CD44, were analyzed for apoptosis by flow cytometry using either the annexin V–fluorescein isothiocyanate (BD Bioscience, catalog no. 556547) or annexin V–APC (eBioscience, catalog no. 88-8007-74) Apoptosis Detection kit in TER119$^+$CD45$^-$ erythroblasts. FACS sorted erythroblasts of indicated stages stained with TER119 and CD44 were washed, and resuspended in 100 μL 1× annexin V binding buffer, and stained with annexin V for 15 minutes followed by 7-aminoactinomycin D or PI staining, per the manufacturer's instructions. Apoptotic cells were then analyzed within 1 hour.

Ki-67 staining

FACS purified erythroblasts of indicated stages were isolated from WT, *p21*$^{-/-}$, *Hbb*$^{th3/+}$, and *p21*$^{-/-}$/*Hbb*$^{th3/+}$ mice and stained for Ki-67 using the Mouse Anti-Ki-67 Set (BD Biosciences, catalog no. 556026). Briefly, cells were fixed in 70% ethanol at −20°C for 2 hours. These were then washed twice at 500 g for 10 minutes with PBS supplemented with 1% FBS and 0.09% sodium azide, and resuspended at a concentration of a million cells per 100 μL. After transferring into a fresh tube, 20 μL antibody was added, gently mixed, and incubated at room temperature for 20 to 30 minutes in the dark. After 2 washes with PBS at 500 g for 5 minutes, the supernatant was discarded, the cells were resuspended in 500 μL PBS, and 10 μL of PI solution was added. FACS analysis was carried out using the BD LSRII instrument.

Immunofluorescence staining and confocal microscopy

FACS-sorted erythroid progenitor (TER119$^-$, c-KIT$^+$, and CD71^{Hi}) cells from the bone marrow of WT, *Hbb*$^{th3/+}$, *p21*$^{-/-}$, and *p21*$^{-/-}$/*Hbb*$^{th3/+}$ mice were cytospun at 250 rpm for 3 minutes. These were then fixed with 4% paraformaldehyde (Alfa Aesar by ThermoFisher Scientific, catalog no. 43368) and permeabilized with 0.1% Triton X-100/1× PBS solution. After blocking in 1% BSA/1× PBS solution for 1 hour, the slides were incubated with the primary antibodies overnight (anti-TP53 and anti-FOXO3). The slides were then washed 3 times with 1× PBS and incubated at room temperature for 1 hour with the secondary antibody. The slides were again washed 3 times with 1× PBS, air dried, and mounted with Fluoroshield mounting medium containing DAPI (Abcam, catalog no. ab104139). Antibodies used: CD71-PE (BD Biosciences, catalog no. 553267), c-KIT-APC (BD Biosciences, catalog no. 553356), TP53 (Santa Cruz Biotechnology, catalog no. sc-126 or Cell Signaling, catalog no. 2524), and FOXO3 (Cell Signaling).

Microscopy image analysis

Fluorescence intensity was quantified using ImageJ for 30 to 50 individual cells per experiment group. The channels were first split from merged channel images and "Raw Integrated Density" (RawIntDen) of selected channel (protein of interest) was measured by the "Measure" command. To quantify nuclear mean fluorescence intensity, nuclear area was first defined by the threshold set in the DAPI channel and mapped to the selected channel as "Area of Interest" (AOI). Nuclear mean fluorescence intensity was then measured using the "Mean" function (RawIntDen of AOI divided by the area size of AOI).

Human CD34 purification and culture

Peripheral blood was obtained from healthy controls and patients with β-thalassemia (institutional review board: 15-012123, The Children's Hospital of Philadelphia [CHOP], Stefano Rivella) and CD34$^+$ cells were isolated by positive selection using the human CD34 Microbead kit from Miltenyi Biotec (catalog no.130-046-702) as per the manufacturer's instructions. The CD34 culture and differentiation was performed as previously described.[29,47] CD235a (glycophorin A), CD49d (α4 integrin), and CD233

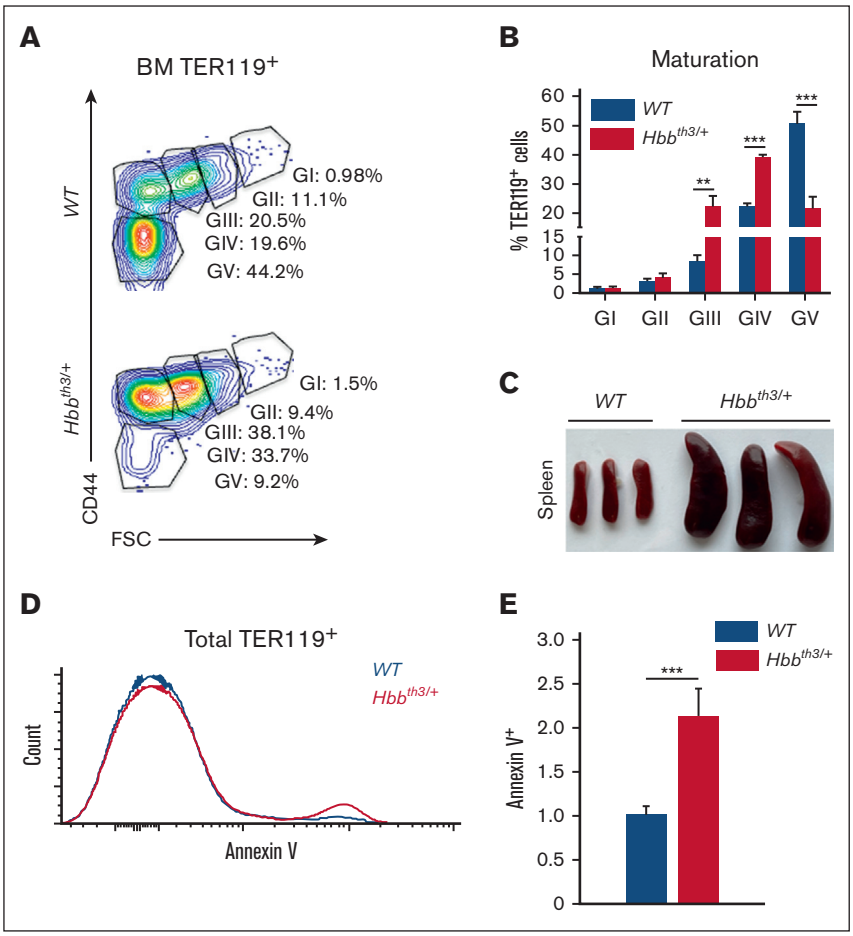

Figure 1. Erythroid apoptosis in β-thalassemia (*Hbb*$^{th3/+}$) mice. (A) Gating strategy to identify pro-, basophilic, polychromatophilic erythroblasts (gate [G] I-GIII), orthochromatic erythroblasts and reticulocytes (GIV), and RBCs (GV) in WT and *Hbb*$^{th3/+}$ bone marrow (BM) cells. (B) Graphs showing the percentage of each population in panel A. Note the increased gate III and IV with a concomitant decrease in gate V *Hbb*$^{th3/+}$ erythroid cells. (C) Macroscopic appearance of the spleen in WT and *Hbb*$^{th3/+}$ mice. (D) Overlay of FACS histogram of annexin V staining of WT vs *Hbb*$^{th3/+}$ BM TER119^{+} subpopulations in live cells. (E) Fold change of annexin V^{+} in live TER119^{+} *Hbb*$^{th3/+}$ relative to WT cells (n ≥ 3). Results are shown as mean ± standard deviation (SD); $^{**}P < .01$, $^{***}P < .001$.

(band 3) antibodies were obtained from Xiuli An's laboratory (New York Blood Center) and used for determining the stage of erythroid cell differentiation, as previously described.[29] The protocol was in accordance with the Declaration of Helsinki.

Quantitative reverse transcription polymerase chain reaction (qRT-PCR) analysis

Total RNA was isolated using the RNeasy Mini kit (Qiagen, catalog no. 74004). qRT-PCR analysis was carried out as described previously.[14,27]

Statistics

Student unpaired 2-tailed *t* test was carried out for all experiments unless specified otherwise. Error bars indicate standard deviation or standard error, as indicated in the figure legends. The number of mice used (sample size) is mentioned in the figure legends. Each experiment was repeated at least 3 times independently with 2 or 3 technical replicates unless specified otherwise. All statistical analyses were carried out using the GraphPad Prism software.

Results

Apoptotic phenotype in mouse β-thalassemia is similar to human β-thalassemia

To address the underlying mechanism of apoptosis of β-thalassemic erythroid cells, we used *Hbb*$^{th3/+}$ mice that are heterozygous for deleted β1 and β2 globin subunits and exhibit a phenotype similar to that of human β-thalassemia intermedia.[44,48] Using flow cytometry analysis of erythroid cell maturation with parameters of size (forward scatter), CD44, and TER119 markers,[49] we found that the anemia-associated erythroblasts decreased in RBCs in gate V. In addition, heterozygous *Hbb*$^{th3/+}$ erythroblasts[44,48] show an increase in polychromatophilic and orthochromatic erythroblasts found in gates III and IV (Figure 1A-B). Similar to patients with β-thalassemia, *Hbb*$^{th3/+}$ mice display splenomegaly, which results from extramedullary erythropoiesis associated with clearing damaged RBCs (Figure 1C). Elevated ROS levels suggesting increased oxidative damage were also observed in late maturing β-thalassemic erythroid cells and mirror features of human β-thalassemia (supplemental Figure 1A). Interestingly, ROS levels were not significantly different in the β-thalassemia erythroid progenitor compartment as compared with that of WT controls (supplemental Figure 1B).

To further validate the model independently, we determined that the frequency of apoptotic (annexin V^{+}) bone marrow erythroblasts within the viable fraction is significantly higher in *Hbb*$^{th3/+}$ relative to WT live erythroblasts (Figure 1D-E; supplemental Figure 2), similar to what has been observed in patients with β-thalassemia.[5]

FOXO3 is activated prematurely in the β-thalassemic erythroid compartment

To evaluate whether FOXO3 is implicated in regulating β-thalassemic erythroid apoptosis, FOXO3 expression and nuclear localization,

Table 1. Blood parameters in *Hbb*$^{th3/+}$ vs *Foxo3*$^{-/-}$/*Hbb*$^{th3/+}$

Parameters	WT	*Foxo3*$^{-/-}$	*Hbb*$^{th3/+}$	*Foxo3*$^{-/-}$/*Hbb*$^{th3/+}$
RBC (10^9/L)	10 400 ± 300	9000 ± 100*	6700 ± 700*	7500 ± 600†
HGB (g/dL)	15.0 ± 0.3	14.8 ± 0.1	8.2 ± 0.3*	9.2 ± 0.7†
HCT (%)	54.6 ± 1.6	52.8 ± 0.9	29.3 ± 5.2*	34.5 ± 3.9†
MCV (fL)	52.8 ± 1.2	58.5 ± 0.8*	41.2 ± 1.4*	45.1 ± 3.0†
MCH (pg)	14.6 ± 0.2	16.4 ± 0.2	12.7 ± 1.6*	12.5 ± 0.4
MCHC (g/dL)	27.4 ± 0.5	28.0 ± 0.3	30.2 ± 4.1	27.2 ± 1.4†
Retic (%)	3.6 ± 0.3	6.6 ± 0.5*	24.0 ± 5.7*	28.3 ± 7.0
n (mice)	9	10	7	10

HCT, hematocrit; HGB, hemoglobin; MCH, mean corpuscular hemoglobin; MCHC, MCH concentration; MCV, mean corpuscular volume; Retic, reticulocytes.
*$P < .05$ between WT and *Foxo3*$^{-/-}$ or *Hbb*$^{th3/+}$.
†$P < .05$ between *Hbb*$^{th3/+}$ and *Foxo3*$^{-/-}$/*Hbb*$^{th3/+}$.

indications of FOXO3 activity, were analyzed (supplemental Figure 3) in erythroid progenitors and early erythroblasts before exhibiting apoptosis. These populations were identified as TER119$^-$, c-KIT$^+$, CD71^{Hi} cells and to contain both burst forming unit–erythroid (BFU-e) cells and colony forming unit–erythroid (CFU-e) cells[50,51] (supplemental Figure 3A). As anticipated, the erythroid progenitor compartment (TER119$^-$, c-KIT$^+$, CD71^{Hi}) was expanded while there was no difference in TER119$^-$, c-KIT$^+$, CD71^{LO} in β-thalassemic mice (supplemental Figure 3A). *Foxo3* transcripts were elevated in *Hbb*$^{th3/+}$ relative to in WT early erythroblasts (supplemental Figure 3B). FOXO3 protein expression in the nucleus was also enhanced in erythroid progenitor (TER119$^-$, c-KIT$^+$, CD71^{Hi})[50] cells as measured by immunofluorescence analysis (supplemental Figure 3C). Together, these results indicate that FOXO3 is activated prematurely in β-thalassemic erythroid progenitors.

Because the proapoptotic TP53 is in a regulatory network with FOXO3,[31,37] we examined the status of TP53 in *Hbb*$^{th3/+}$ erythroblasts. Immunofluorescence staining also detected a similar pattern of slight increased nuclear TP53 protein expression, trending higher in *Hbb*$^{th3/+}$ TER119$^-$, c-KIT$^+$, CD71^{Hi} [50] progenitors compared with in WT controls, albeit the difference was not statistically significant (supplemental Figure 4). Together, these studies suggest that FOXO3 may mediate the increased apoptosis in *Hbb*$^{th3/+}$ erythroblasts.

Loss of FOXO3 reduces erythroblast apoptosis and improves RBC production in a β-thalassemia mouse model

To further dissect the role of FOXO3 in the pathophysiology of β-thalassemia, we generated double-mutant *Foxo3*$^{-/-}$/*Hbb*$^{th3/+}$ mice. In agreement with FOXO3 mediation of erythroid cell apoptosis, loss of FOXO3 in *Hbb*$^{th3/+}$ mice improved the anemia (Table 1; Figure 2A), with an observed increase in RBC production by ~10%, and in hemoglobin content by 1g/dL (Table 1). These significant results were notable specifically in the context of β-thalassemia. Importantly, apoptosis was markedly reduced in *Foxo3*$^{-/-}$/*Hbb*$^{th3/+}$ erythroblasts (Figure 2B; supplemental Figure 5A). These results were specific to loss of *Foxo3* and not due to a FOXO1 compensation in *Foxo3*-deleted cells, given the absence of any significant upregulation of *Foxo1* transcript that encodes for the other FOXO protein that is expressed in erythroid cells (supplemental Figure 5B) and that shares targets with FOXO3.[17,36] Together these results suggest that FOXO3 upregulation is proapoptotic in the β-thalassemic erythroid compartment. However, loss of FOXO3 did not rescue the splenomegaly in *Hbb*$^{th3/+}$ mice, indicating persistent extramedullary hematopoiesis (Figure 2C). In agreement with the FOXO3 antioxidant functions,[17,30] ROS levels were increased in the bone marrow (supplemental Figure 6A) and spleen (supplemental Figure 6B) of double-mutant *Foxo3*$^{-/-}$/*Hbb*$^{th3/+}$ relative to *Hbb*$^{th3/+}$ erythroblasts, suggesting that improved erythroblast survival in *Foxo3*$^{-/-}$/*Hbb*$^{th3/+}$ mice was despite increased ROS accumulation in erythroid compartments of double-mutant mice (supplemental Figure 6). These findings also support the notion that the upregulated FOXO3 mitigates ROS accumulation in β-thalassemic erythroblasts. Furthermore, these results indicate that the apoptotic phenotype in β-thalassemic erythroblasts, and its alleviation in *Foxo3*$^{-/-}$/*Hbb*$^{th3/+}$ erythroblasts (Figure 2; supplemental Figures 5 and 6), are likely independent of oxidative stress.

Earlier studies have shown FOXO3 to be key in regulating cell cycle in addition to apoptosis in a context- and stress-dependent manner.[17,18,20,21,27,30,36,46,52] RNA-sequencing analyses[14] revealed deregulated expression of many apoptotic genes in *Foxo3*$^{-/-}$ erythroblasts relative to WT controls (supplemental Figure 7A, previously published RNA-sequencing analyses[14]). Furthermore, using a Fluidigm Platform we interrogated the expression of a panel of apoptotic genes by qRT-PCR analysis in double-mutant *Foxo3*$^{-/-}$/*Hbb*$^{th3/+}$ erythroblasts. Among these, we found that the expression of BCL2 family member p53 up-regulated modulator of apoptosis (PUMA) transcript and protein, but not Bcl-2 Interacting Mediator of cell death (BIM; also known as Bcl-2-like protein 11; BCL2L11), both targets of FOXO3 and TP53,[53,54] was greatly augmented in *Hbb*$^{th3/+}$ erythroblasts (supplemental Figure 7B-C). Notably, PUMA's expression was significantly downregulated in double-mutant *Foxo3*$^{-/-}$/*Hbb*$^{th3/+}$ erythroblasts (supplemental Figure 7B). However, generating double-mutant *Puma*$^{-/-}$/*Hbb*$^{th3/+}$ erythroblasts by crossbreeding was not productive, likely because of the linkage of *Puma* and *β-globin* genes on mouse chromosome 7, thus excluding the possibility to further examine the physiological role of PUMA as a mediator of β-thalassemic erythroid apoptosis using this approach.

P21 ablation reduces β-thalassemia erythroid apoptosis without significantly improving RBC formation

Next, we focused on P21,[55] which is another common target of both FOXO3 and TP53.[17,30,31,56,57] We found that *p21* transcripts were significantly upregulated in *Hbb*$^{th3/+}$ erythroblasts throughout maturation (Figure 3A). P21 protein expression was also greatly enhanced in mouse *Hbb*$^{th3/+}$ erythroblasts (Figure 3B). Importantly, expression of P21 protein was also significantly elevated in human erythroblasts differentiated from CD34$^+$ cells derived from patients with β-thalassemia (n = 2), strongly suggesting conservation of P21 upregulation between mouse and human β-thalassemic erythroblasts and potential pathological mechanisms (Figure 3C-D).

Given that under certain stress conditions, P21 regulates apoptosis in addition to inhibiting cell cycle,[55,58] we addressed the potential contribution of P21 to the enhanced apoptosis by generating *p21*$^{-/-}$/*Hbb*$^{th3/+}$ mice. We opted for an in vivo approach to avoid the

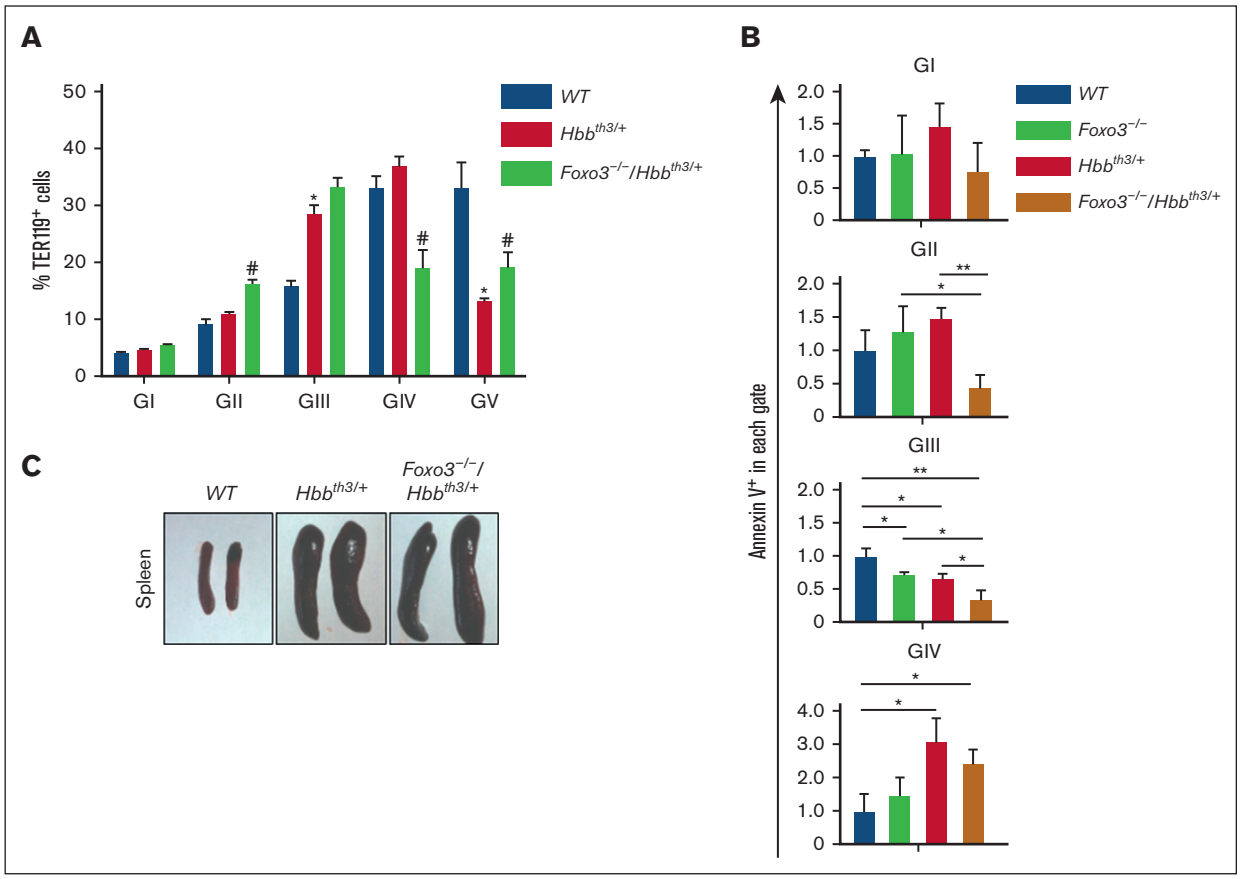

Figure 2. Loss of FOXO3 improves RBC production in β-thalassemia. (A) FOXO3 ablation alters BM erythroblast frequencies. *$P < .05$ between WT and *Hbb*$^{th3/+}$ groups and #$P < .05$ between *Hbb*$^{th3/+}$ and *Foxo3*$^{-/-}$/*Hbb*$^{th3/+}$ groups (n ≥ 3). (B) Fold change of annexin V$^+$ cells in live *Foxo3*$^{-/-}$, *Hbb*$^{th3/+}$, and *Foxo3*$^{-/-}$/*Hbb*$^{th3/+}$ relative to WT BM TER119$^+$ cells in each gate. *$P < .05$, **$P < .01$. (C) Macroscopic examination of the spleen from WT, *Hbb*$^{th3/+}$, and *Foxo3*$^{-/-}$/*Hbb*$^{th3/+}$. Results are shown as mean ± SD.

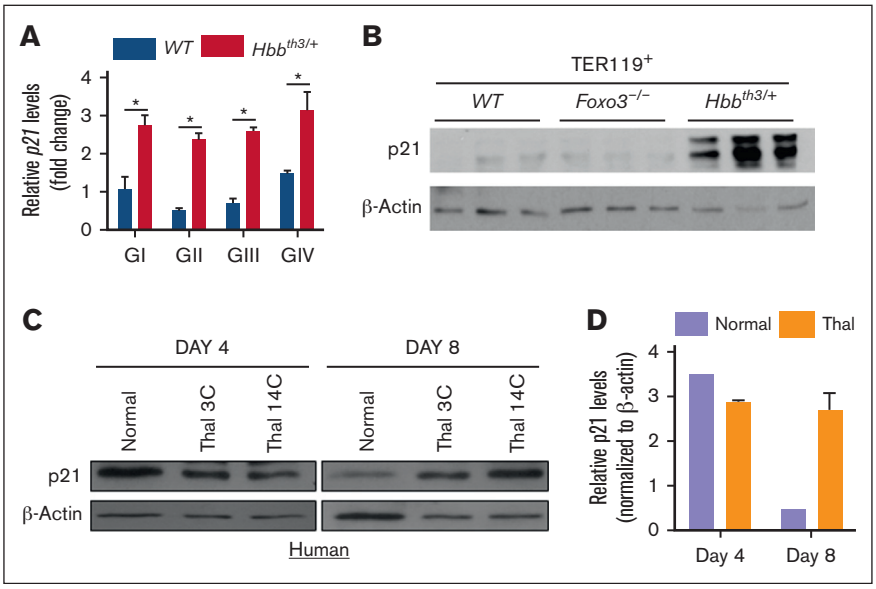

Figure 3. P21 is upregulated in β-thalassemia erythroid cells. (A) qRT-PCR expression analysis of P21 in TER119$^+$ (GI-GIV) cells. (B) Immunoblotting of P21 protein expression in WT, *Foxo3*$^{-/-}$, and *Hbb*$^{th3/+}$ TER119$^+$ erythroblasts. Results are shown as mean ± SD; *$P < .05$ (n = 3 mice). (C) Immunoblot analysis of P21 expression in erythroblasts derived from healthy donors and CD34$^+$ cells from patients with β-thalassemic. (D) Quantification of data shown in panel C.

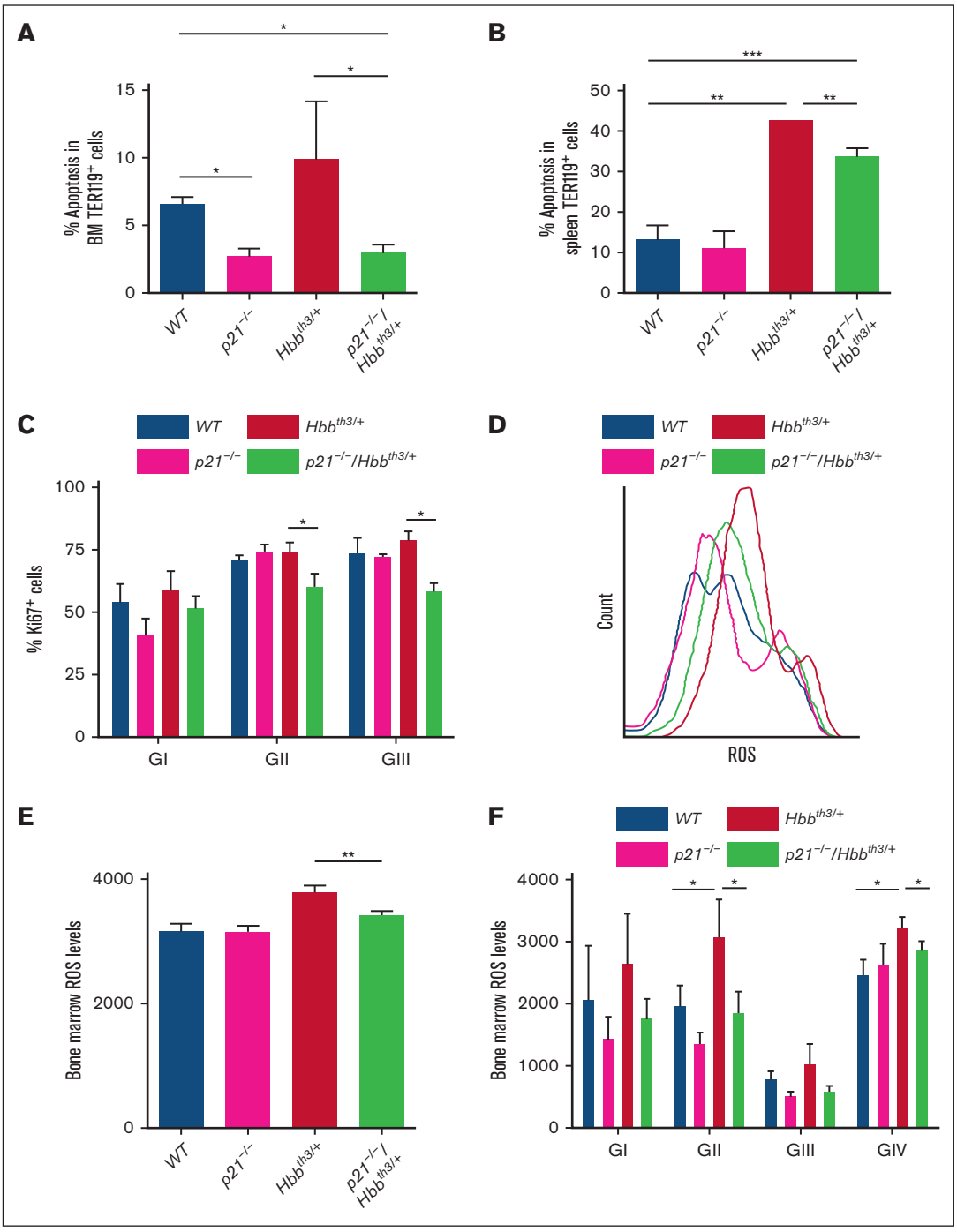

Figure 4. Loss of P21 reduces apoptosis of β-thalassemia erythroid cells. (A) Flow cytometric analysis of apoptosis in BM erythroid cells. *$P < .05$ between $Hbb^{th3/+}$ and $p21^{-/-}/Hbb^{th3/+}$, and between $p21^{-/-}$ or $p21^{-/-}/Hbb^{th3/+}$ and WT groups (n = 3 mice for each group). (B) Flow cytometric analysis of apoptosis in splenic erythroid cells. **$P < .01$ between $Hbb^{th3/+}$ and $p21^{-/-}/Hbb^{th3/+}$, and between $Hbb^{th3/+}$ and WT groups; ***$P < .001$ between $p21^{-/-}/Hbb^{th3/+}$ and WT groups (n = 3 mice for each group). (C) Flow cytometric analysis of cell proliferation in BM erythroid cells. *$P < .05$ between $Hbb^{th3/+}$ and $p21^{-/-}/Hbb^{th3/+}$groups (n = 3 for each group). (D) Histogram of ROS levels in total BM erythroblasts ($TER119^{+}$) as measured by CM-H_2DCFDA probe; and quantification in (E). **$P < .01$ between $Hbb^{th3/+}$ and $p21^{-/-}/Hbb^{th3/+}$ groups (n = 3). (F) ROS levels in BM-erythroblast populations within GI to GIV obtained from indicated groups of mice. *$P < .05$ between $Hbb^{th3/+}$ and $p21^{-/-}/Hbb^{th3/+}$, and between $Hbb^{th3/+}$ and WT groups. All results are shown as mean ± SD.

impending artifacts of in vitro targeting on erythroblast maturation and apoptosis.[59] The double-mutant $p21^{-/-}/Hbb^{th3/+}$ mice were born following a non-Mendelian pattern and only a small subset survived to the adulthood. The subsequent experiments were carried using this $p21^{-/-}/Hbb^{th3/+}$ adult group. We found that loss of P21 on a β-thalassemic background significantly alleviated apoptosis as observed in $p21^{-/-}/Hbb^{th3/+}$ relative to $Hbb^{th3/+}$ bone marrow erythroblasts (Figure 4A; n = 6) and to a lesser extent in the spleen

Table 2. Blood parameters in $Hbb^{th3/+}$ vs $p21^{-/-}/Hbb^{th3/+}$

Parameters	WT	$p21^{-/-}$	$Hbb^{th3/+}$	$p21^{-/-}/Hbb^{th3/+}$
RBC (10^9/L)	10 500 ± 900	10 500 ± 300	7900 ± 900†	8200 ± 400
HGB (g/dL)	15.4 ± 1.1	15.3 ± 0.3	8.5 ± 0.8†	8.8 ± 0.4
WBC 10^3/μL	4.3 ± 2.2	5.3 ± 1.9	14.9 ± 6.7†	9.0 ± 3.9‡
Lympho (K/μL)	3.3 ± 1.9	3.6 ± 1.9	11.3 ± 5.9†	6.7 ± 2.9‡
EO (K/μL)	0.10 ± 0.11	0.11 ± 0.09	0.23 ± 0.15	0.18 ± 0.17
Retic (%)	3.8 ± 0.5	3.6 ± 0.5	28.4 ± 2.0†	28 ± 4.1
n (mice)	9	6	7	6

EO, eosinophils; HGB, hemoglobin; Lympho, lymphocytes; WBC, white blood cells.
†$P < .01$ between WT and $Hbb^{th3/+}$.
‡$P < .05$ between $Hbb^{th3/+}$ and $p21^{-/-}/Hbb^{th3/+}$.

erythroblasts (Figure 4B; supplemental Figure 8), suggesting that, indeed, upregulated P21 mediates apoptosis in the β-thalassemic erythroblasts. Despite P21 being a potent inducer of cell cycle arrest, the decrease in apoptosis was associated with significantly reduced cycling of $p21^{-/-}/Hbb^{th3/+}$ relative to $Hbb^{th3/+}$ erythroblasts, as evidenced by Ki67 cell cycle marker (Figure 4C). Combined with decreased cell cycling, ROS levels were also reduced in the $p21^{-/-}/Hbb^{th3/+}$ relative to $Hbb^{th3/+}$ bone marrow erythroblasts and almost normalized to WT levels (Figure 4D-F). Unexpectedly however, even with decreased bone marrow apoptosis and improved erythroblast survival, loss of P21 did not ameliorate erythroid cell production in β-thalassemic mice (supplemental Figures 8A-G and 9; Table 2). RBC numbers, reticulocytosis, and related parameters in $p21^{-/-}/Hbb^{th3/+}$ mice relative to $Hbb^{th3/+}$ mice were not significantly different (Table 2). Although loss of P21 led to reduced circulating EPO (supplemental Figure 8I) that signals the improvement of $Hbb^{th3/+}$ erythropoiesis, it did not alleviate the splenomegaly, extramedullary erythropoiesis (supplemental Figure 8A-B), or elevated ROS levels in β-thalassemic spleen erythroblasts (supplemental Figure 8A-I; Table 2). Altogether these results suggest that reducing apoptosis in β-thalassemic erythroblasts does not improve RBC production or attenuate ineffective erythropoiesis.

Decreased cycling of $p21^{-/-}/Hbb^{th3/+}$ relative to $Hbb^{th3/+}$ erythroblasts was surprising. To gain further insight into mechanisms that regulate $p21^{-/-}/Hbb^{th3/+}$ cycling, we analyzed $p21^{-/-}/Hbb^{th3/+}$ erythroblasts by confocal microscopy immunofluorescence staining for the expression of FOXO3 and TP53 because these proteins both regulate erythroid cell cycling[17] (Figure 5A). Although FOXO3 nuclear expression was substantially enhanced in $p21^{-/-}/Hbb^{th3/+}$ $TER119^{-}$ $c\text{-}KIT^{+}$, $CD71^{Hi}$ cells, indicating FOXO3 activation in precursors upstream of the formation of erythroblasts (Figure 5Ai), in contrast, we observed that the nuclear expression of TP53 protein had decreased specifically in these double-mutant erythroblast precursors relative to controls (Figure 5Aii). These studies suggest that the upregulated FOXO3, and possibly FOXO3-reduction of ROS levels, are likely mediating the cell cycle inhibition in $p21^{-/-}/Hbb^{th3/+}$ erythroblasts. In addition, these results identify the interplay between P21, FOXO3, and TP53 in regulating $Hbb^{th3/+}$ erythroblast cycling and apoptosis. To explore the mechanism of reduced ROS levels in $p21^{-/-}/Hbb^{th3/+}$ erythroblasts, and considering that FOXO3 is implicated in regulating mitochondria[45,60,61] and ROS levels,[17,30,46,62,63] we analyzed mitochondrial parameters that modify, and respond to, levels of ROS and cell cycle stage.[64-66] We found that mitochondrial network fusion is significantly increased in $Hbb^{th3/+}$ vs WT erythroblasts as analyzed by Mitotracker Green (Figure 5B). We further found that mitochondrial fragmentation was markedly increased in $p21^{-/-}/Hbb^{th3/+}$ even as compared with $Hbb^{th3/+}$ erythroblasts, especially in gate III (Figure 5C). These findings were unexpected because mitochondrial fragmentation is often associated with apoptosis. However, these findings may explain the reduced ROS levels and cell cycling in $p21^{-/-}/Hbb^{th3/+}$ erythroblasts. Thus, the increase in mitochondrial fragmentation is associated with cell cycle inhibition, reduced ROS levels, and decreased apoptosis in $p21^{-/-}/Hbb^{th3/+}$ relative to $Hbb^{th3/+}$ erythroblasts.

Discussion

Here, we found that P21 (CDKN1A) expression is upregulated in both mouse and human β-thalassemic erythroid cells; we further showed that the elevated P21 mediates apoptosis in adult β-thalassemic $Hbb^{th3/+}$ bone marrow and, to a much lesser extent, spleen erythroid cells. Notably, given that loss of P21 is not lethal in mice,[67,68] the in utero death of $p21^{-/-}/Hbb^{th3/+}$ mice suggests that the upregulated P21 expression is necessary for the survival of β-thalassemic $Hbb^{th3/+}$ embryos. Our results indicate that, paradoxically, the greatly enhanced P21 expression supports β-thalassemic erythroblast cell cycling (Figure 4C). P21 functions in a molecular network with FOXO3 and TP53, that are both transcriptional regulators of cell cycle inhibition and apoptosis.[36,69-72]

The cyclin-dependent kinase inhibitor P21 is mostly known for its function in cell cycle arrest through regulation of cyclin-dependent kinase proteins.[55] In addition, many complex functions are attributed to P21, including both proapoptotic and antiapoptotic properties.[55,73-75] The proapoptotic function of P21 is TP53 dependent or independent, and mediators of proapoptotic P21 function are poorly defined.[72] Our genetic studies identify proapoptotic functions for P21 in the context of β-thalassemic erythropoiesis, and also provide evidence supporting the notion that P21 mediates apoptosis in a TP53-independent manner.

Our results also identify FOXO3 as a mediator of β-thalassemic erythroid apoptosis, presumably upstream of P21, although we did not address this directly in the context of β-thalassemia. FOXO3 is upregulated in the $Hbb^{th3/+}$ erythroid compartment in which P21 is elevated (and TP53 is not downregulated). Loss of P21 is associated with upregulated FOXO3 but also notably decreased TP53 expression in the erythroid compartment. Loss of FOXO3 clearly improved RBC production in $Hbb^{th3/+}$ β-thalassemic mice. This improvement was significant in the context of β-thalassemia, with a gain of 1 g/dL of hemoglobin (as in $Foxo3^{-/-}/Hbb^{th3/+}$ erythroblasts), equivalent to 1 unit of blood, may notably reduce the transfusion schedule in patients with β-thalassemia. Given the erythroid phenotype in $Foxo3^{-/-}$ mice,[17,27] these results were unanticipated. We had previously found that loss of FOXO3 results in increased circulating EPO and ROS-mediated constitutive activation of both protein kinases Janus kinase 2 and mammalian target of rapamycin complex 1 that sustain EPO receptor signaling and cell growth.[27] In addition, we had shown that inhibiting Janus kinase 2[43] or mammalian target of rapamycin complex 1 with rapamycin[27] improves RBC production and reduces anemia in

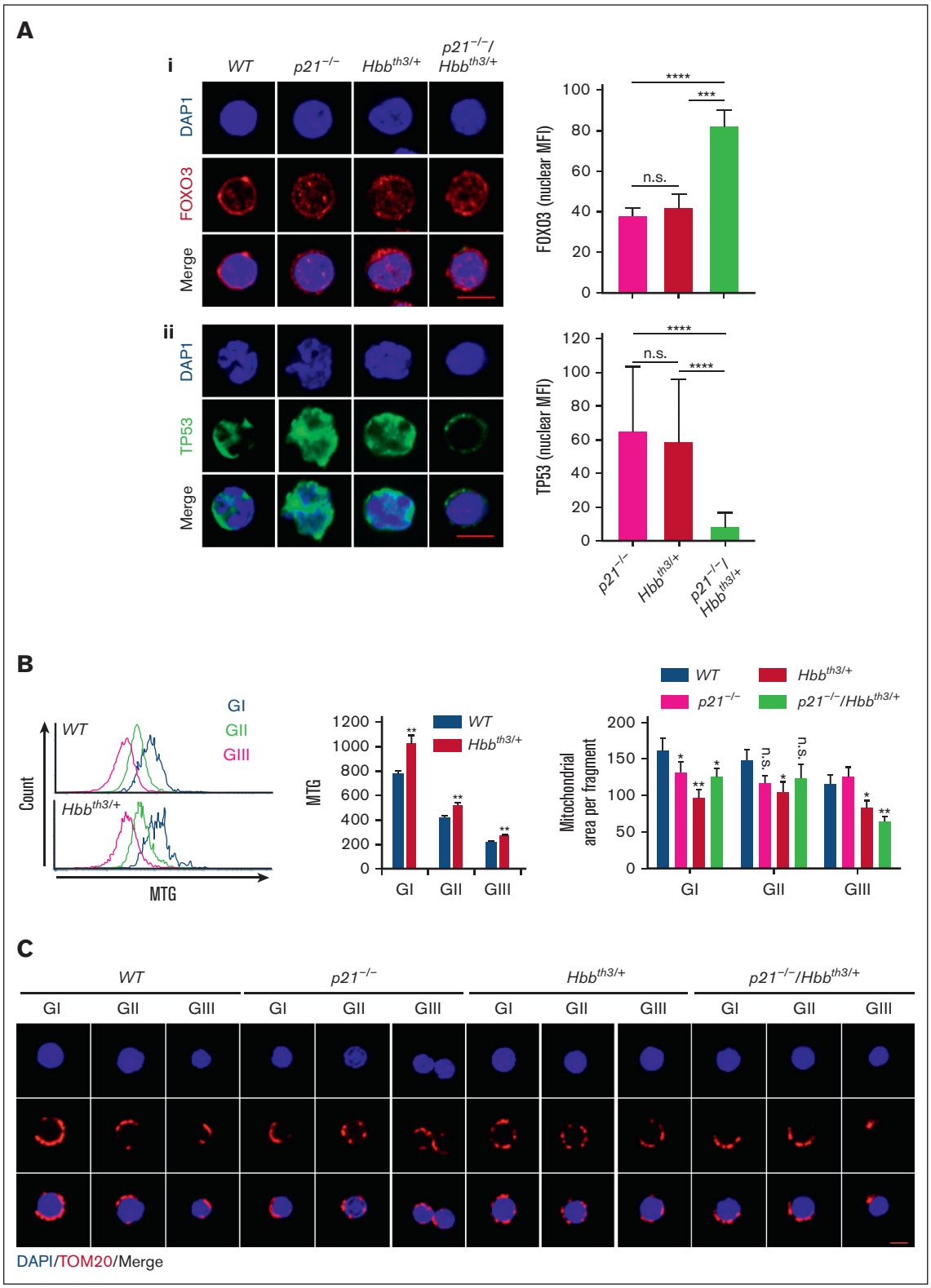

Figure 5. Modulation of FOXO3 and TP53 expression in *p21*$^{-/-}$/*Hbb*$^{th3/+}$ erythroid cells. (Ai) FOXO3 nuclear localization in erythroid progenitors from WT, *p21*$^{-/-}$, *Hbb*$^{th3/+}$, and *p21*$^{-/-}$/*Hbb*$^{th3/+}$ mice using confocal microscopy; analyses of at least 40 cells (quantification, right graph). Scale bar: 5 µm. (Aii) TP53 nuclear localization in erythroid progenitors from WT, *p21*$^{-/-}$, *Hbb*$^{th3/+}$, and *p21*$^{-/-}$/*Hbb*$^{th3/+}$ mice using confocal microscopy; analyses of at least 40 cells (quantification, right graph). Scale bar: 5 µm. (B) Histograms of Mitotracker Green staining of TER119^{+} cells in different gates (left) and quantification (right). (C) Mitochondrial morphology in erythroid progenitors from WT, *p21*$^{-/-}$, *Hbb*$^{th3/+}$, and *p21*$^{-/-}$/*Hbb*$^{th3/+}$ mice using confocal microscopy; analyses of at least 30 cells. Scale bar: 5 µm. Quantification of mitochondrial area (top). Results are shown as mean ± standard error of the mean; *$P < .05$; **$P < .01$; ***$P < .001$; ****$P < .0001$; and n.s., not significant.

$Hbb^{th3/+}$ β-thalassemic mice.[27] However, decreased apoptosis, increased survival of $Foxo3^{-/-}/Hbb^{th3/+}$ erythroblasts (Figure 2B; supplemental Figure 5), and improved RBC production (Table 1; Figure 2A) had no impact on reticulocytosis or splenomegaly; suggesting that either the increased apoptosis is downstream of ineffective erythropoiesis in β-thalassemic mice (Table 1), apoptosis alone is insufficient to sustain β-thalassemic ineffective erythropoiesis, or, alternatively, mechanisms other than apoptosis drive β-thalassemic ineffective erythropoiesis. Because FOXO3's function is critical to RBC production and reticulocyte maturation,[17,19] including mitochondrial removal and enucleation,[14,27] the quality of RBC formed in $Foxo3^{-/-}/Hbb^{th3/+}$ mice may be compromised or, at best, suboptimal. Thus, the potential benefits of targeting FOXO3 has to be first carefully examined before considering using this approach for improving RBC production in β-thalassemia therapies.

Overall, our results showed that reducing apoptosis and significantly improving $Hbb^{th3/+}$ erythroblast survival does not ameliorate poor RBC production (in $p21^{-/-}/Hbb^{th3/+}$ mice) nor reduces the extramedullary erythropoiesis in the β-thalassemic $Hbb^{th3/+}$ mouse model ($p21^{-/-}/Hbb^{th3/+}$ or $Foxo3^{-/-}/Hbb^{th3/+}$ mice). The combination of reduced apoptosis and erythroid cell division results in no gain in RBC numbers or in reducing reticulocytosis in $p21^{-/-}/Hbb^{th3/+}$ mice. Notably, loss of P21 in $Hbb^{th3/+}$ mice had a much lesser effect on the splenic erythroid cells, including spleen apoptosis (reduction by >75% in apoptosis of bone marrow $CD45TER119^{+}$ cells vs <25% in the spleen in $p21^{-/-}/Hbb^{th3/+}$ vs $Hbb^{th3/+}$ mice), erythroid cell numbers, and ROS levels. The lack of improvement observed in the spleen occurred despite reduced EPO levels, suggesting distinct regulation of β-thalassemic erythroid cell maturation in the spleen vs the bone marrow. Reduced ROS levels with the loss of P21 was not associated with improved β-thalassemia RBC production or erythroblast survival in the spleen (Figures 4 and 5; supplemental Figures 8 and 9). These findings indicate that, although increased apoptosis is associated with the expansion of the erythroblast pool, in this β-thalassemic $Hbb^{th3/+}$ mouse model, it is likely that apoptosis is not the main driver of β-thalassemic erythroid cell expansion in the β-thalassemic $Hbb^{th3/+}$ mouse model. Altogether, these findings raise the possibility that ineffective erythropoiesis and apoptosis in β-thalassemia are uncoupled, at least in mice (see "Graphical abstract"). Specifically, reduced/elimination of apoptosis in the bone marrow does not significantly affect β-thalassemic extramedullary hematopoiesis or splenomegaly (in both $p21^{-/-}/Hbb^{th3/+}$ and $Foxo3^{-/-}/Hbb^{th3/+}$ mouse models).

Our findings suggest that the spleen is critical in regulating β-thalassemic erythroid cell survival in the mouse; these data also highlight the differences in the kinetics of erythroid cell maturation, survival, and ROS levels in the spleen vs bone marrow under homeostasis and in the context of β-thalassemia. These findings further support the idea that the microenvironment, including macrophages,[76,77] modulate gene regulation, and is critical in controlling β-thalassemic erythropoiesis.[78,79] Although apoptosis may contribute to ineffective erythropoiesis, apoptosis does not explain the extent of the β-thalassemic erythroid defect. Studies of macrophages, iron overload, and ROS regulation may reveal mechanistic regulations of ineffective erythropoiesis in β-thalassemia that are distinct from apoptosis.

Our findings indicate that a network of P21, FOXO3, and TP53 coordinates erythroid cell cycling and apoptosis in β-thalassemia mice in an unanticipated fashion, presumably to balance cell cycle and apoptosis.

Acknowledgments

The authors thank the Flow Cytometry Core and Microscopy CoRE at the Icahn School of Medicine at Mount Sinai for technical help, Miriam Merad and Yelena Ginzburg (Mount Sinai) for providing $p21^{-/-}$ mice and a subset of $Hbb^{th3/+}$ mice respectively, and Xiuli An (New York Blood Center) for providing antihuman erythroid antibodies and protocol inputs. R.L. was partially supported by an American Heart Association Fellowship and National Institutes of Health grant T32 HD075735 from the Eunice Kennedy Shriver National Institute of Child Health and Human Development.

Work in S.R.'s laboratory is supported by the Commonwealth Universal Research Enhancement Program Pennsylvania, CuRED-Frontier Program, and National Institutes of Health (R01 DK090554 and R01 DK095112). This work was supported by National Institutes of Health (R01HL136255, R01HL61567, and R01CA205975), and funds from New York State Stem Cell Science (NYSTEM) Investigator Initiated Research Projects (IIRP) C32602GG (S.G.).

Authorship

Contribution: R.L. and S.G. designed experiments; R.L., M.L., V.M., J.Q., A.M., and T.A. performed experiments and analyzed data; V.M. prepared figures and assisted in methods; L.B. and S.R. provided samples; and S.G. wrote the manuscript.

Conflict-of-interest disclosure: S.R. is a member of scientific advisory board of Ionis Pharmaceuticals, MeiraGTx, Incyte, and Disc Medicine; owns stock options from Disc Medicine; and has been, or is, a consultant for Cambridge Healthcare Research, Celgene Corporation, Catenion, First Manhattan Co, Forma Therapeutics, Ghost Tree Capital, Keros Therapeutics, Noble Insight, Protagonist Therapeutics, Sanofi Aventis US, Slingshot Insight, Techspert, and Biotechnology Value Fund Partners Limited Partnership, Rallybio, Limited Liability Company, venBio Select LLC. The remaining authors declare no competing financial interests.

The current affiliation for R.L. is Mnemo Therapeutics, New York, NY.

The current affiliation for M.L. is University of Rochester, Rochester, NY.

The current affiliation for V.M. is Department of Therapeutic Radiology, Yale University, New Haven, CT.

ORCID profiles: L.B., 0000-0003-2133-4432; S.R., 0000-0002-0938-6558; S.G., 0000-0002-1835-6107.

Correspondence: Saghi Ghaffari, Department of Cell, Developmental & Regenerative Biology, Icahn School of Medicine at Mount Sinai, Box 1496, New York, NY 10029; email: saghi.ghaffari@mssm.edu.

References

1. Sankaran VG, Nathan DG. Thalassemia: an overview of 50 years of clinical research. *Hematol Oncol Clin North Am*. 2010;24(6):1005-1020.
2. Thein SL. Genetic modifiers of beta-thalassemia. *Haematologica*. 2005;90(5):649-660.
3. Weatherall DJ. Towards molecular medicine; reminiscences of the haemoglobin field, 1960-2000. *Br J Haematol*. 2001;115(4):729-738.
4. Centis F, Tabellini L, Lucarelli G, et al. The importance of erythroid expansion in determining the extent of apoptosis in erythroid precursors in patients with beta-thalassemia major. *Blood*. 2000;96(10):3624-3629.
5. Mathias LA, Fisher TC, Zeng L, et al. Ineffective erythropoiesis in beta-thalassemia major is due to apoptosis at the polychromatophilic normoblast stage. *Exp Hematol*. 2000;28(12):1343-1353.
6. Yuan J, Angelucci E, Lucarelli G, et al. Accelerated programmed cell death (apoptosis) in erythroid precursors of patients with severe beta-thalassemia (Cooley's anemia). *Blood*. 1993;82(2):374-377.
7. Rivella S. Iron metabolism under conditions of ineffective erythropoiesis in beta-thalassemia. *Blood*. 2019;133(1):51-58.
8. Sankaran VG, Weiss MJ. Anemia: progress in molecular mechanisms and therapies. *Nat Med*. 2015;21(3):221-230.
9. Matte A, Federti E, Kung C, et al. The pyruvate kinase activator mitapivat reduces hemolysis and improves anemia in a beta-thalassemia mouse model. *J Clin Invest*. 2021;131(10):e144206.
10. de Franceschi L, Turrini F, Honczarenko M, et al. In vivo reduction of erythrocyte oxidant stress in a murine model of beta-thalassemia. *Haematologica*. 2004;89(11):1287-1298.
11. Franco SS, De Falco L, Ghaffari S, et al. Resveratrol accelerates erythroid maturation by activation of FoxO3 and ameliorates anemia in beta-thalassemic mice. *Haematologica*. 2014;99(2):267-275.
12. Rivella S. Ineffective erythropoiesis and thalassemias. *Curr Opin Hematol*. 2009;16(3):187-194.
13. Ginzburg Y, Rivella S. beta-thalassemia: a model for elucidating the dynamic regulation of ineffective erythropoiesis and iron metabolism. *Blood*. 2011;118(16):4321-4330.
14. Liang R, Camprecios G, Kou Y, et al. A systems approach identifies essential FOXO3 functions at key steps of terminal erythropoiesis. *PLoS Genet*. 2015;11(10):e1005526.
15. Stagg DB, Whittlesey RL, Li X, et al. Genetic loss of Tmprss6 alters terminal erythroid differentiation in a mouse model of beta-thalassemia intermedia. *Haematologica*. 2019;104(10):e442-e446.
16. Matte A, De Falco L, Iolascon A, et al. The interplay between peroxiredoxin-2 and nuclear factor-erythroid 2 is important in limiting oxidative mediated dysfunction in beta-thalassemic erythropoiesis. *Antioxid Redox Signal*. 2015;23(16):1284-1297.
17. Marinkovic D, Zhang X, Yalcin S, et al. Foxo3 is required for the regulation of oxidative stress in erythropoiesis. *J Clin Invest*. 2007;117(8):2133-2144.
18. Bakker WJ, Harris IS, Mak TW. FOXO3a is activated in response to hypoxic stress and inhibits HIF1-induced apoptosis via regulation of CITED2. *Mol Cell*. 2007;28(6):941-953.
19. Bakker WJ, van Dijk TB, Parren-van Amelsvoort M, et al. Differential regulation of Foxo3a target genes in erythropoiesis. *Mol Cell Biol*. 2007;27(10):3839-3854.
20. Pourfarzad F, von Lindern M, Azarkeivan A, et al. Hydroxyurea responsiveness in beta-thalassemic patients is determined by the stress response adaptation of erythroid progenitors and their differentiation propensity. *Haematologica*. 2013;98(5):696-704.
21. Yu D, dos Santos CO, Zhao G, et al. miR-451 protects against erythroid oxidant stress by repressing 14-3-3zeta. *Genes Dev*. 2010;24(15):1620-1633.
22. Uddin S, Kottegoda S, Stigger D, Platanias LC, Wickrema A. Activation of the Akt/FKHRL1 pathway mediates the antiapoptotic effects of erythropoietin in primary human erythroid progenitors. *Biochem Biophys Res Commun*. 2000;275(1):16-19.
23. Komatsu N, Watanabe T, Uchida M, et al. A member of Forkhead transcription factor FKHRL1 is a downstream effector of STI571-induced cell cycle arrest in BCR-ABL-expressing cells. *J Biol Chem*. 2003;278(8):6411-6419.
24. Ghaffari S, Jagani Z, Kitidis C, Lodish HF, Khosravi-Far R. Cytokines and BCR-ABL mediate suppression of TRAIL-induced apoptosis through inhibition of Forkhead FOXO3a transcription factor. *Proc Natl Acad Sci U S A*. 2003;100(11):6523-6528.
25. Eijkelenboom A, Mokry M, de Wit E, et al. Genome-wide analysis of FOXO3 mediated transcription regulation through RNA polymerase II profiling. *Mol Syst Biol*. 2013;9:638.
26. Eijkelenboom A, Mokry M, Smits LM, Nieuwenhuis EE, Burgering BM. FOXO3 selectively amplifies enhancer activity to establish target gene regulation. *Cell Rep*. 2013;5(6):1664-1678.
27. Zhang X, Camprecios G, Rimmele P, et al. FOXO3-mTOR metabolic cooperation in the regulation of erythroid cell maturation and homeostasis. *Am J Hematol*. 2014;89(10):954-963.
28. McIver SC, Kang YA, DeVilbiss AW, et al. The exosome complex establishes a barricade to erythroid maturation. *Blood*. 2014;124(14):2285-2297.
29. Liang R, Menon V, Qiu J, et al. Mitochondrial localization and moderated activity are key to murine erythroid enucleation. *Blood Adv*. 2021;5(10):2490-2504.
30. Yalcin S, Zhang X, Luciano JP, et al. Foxo3 is essential for the regulation of ataxia telangiectasia mutated and oxidative stress-mediated homeostasis of hematopoietic stem cells. *J Biol Chem*. 2008;283(37):25692-25705.

31. You H, Mak TW. Crosstalk between p53 and FOXO transcription factors. *Cell Cycle*. 2005;4(1):37-38.
32. Liang R, Ghaffari S. Advances in understanding the mechanisms of erythropoiesis in homeostasis and disease. *Br J Haematol*. 2016;174(5):661-673.
33. Liang R, Menon V, Ghaffari S. Following transcriptome to uncover FOXO biological functions. *Methods Mol Biol*. 2019;1890:219-227.
34. Liang R, Ghaffari S. Mitochondria and FOXO3 in stem cell homeostasis, a window into hematopoietic stem cell fate determination. *J Bioenerg Biomembr*. 2017;49(4):343-346.
35. Bigarella CL, Li J, Rimmele P, Liang R, Sobol RW, Ghaffari S. FOXO3 transcription factor is essential for protecting hematopoietic stem and progenitor cells from oxidative DNA damage. *J Biol Chem*. 2017;292(7):3005-3015.
36. Salih DA, Brunet A. FoxO transcription factors in the maintenance of cellular homeostasis during aging. *Curr Opin Cell Biol*. 2008;20(2):126-136.
37. Renault VM, Thekkat PU, Hoang KL, et al. The pro-longevity gene FoxO3 is a direct target of the p53 tumor suppressor. *Oncogene*. 2011;30(29):3207-3221.
38. You H, Yamamoto K, Mak TW. Regulation of transactivation-independent proapoptotic activity of p53 by FOXO3a. *Proc Natl Acad Sci U S A*. 2006;103(24):9051-9056.
39. Seoane J, Le HV, Shen L, Anderson SA, Massague J. Integration of Smad and Forkhead pathways in the control of neuroepithelial and glioblastoma cell proliferation. *Cell*. 2004;117(2):211-223.
40. el-Deiry WS, Tokino T, Velculescu VE, et al. WAF1, a potential mediator of p53 tumor suppression. *Cell*. 1993;75(4):817-825.
41. Sieff CA, Yang J, Merida-Long LB, Lodish HF. Pathogenesis of the erythroid failure in Diamond Blackfan anaemia. *Br J Haematol*. 2010;148(4):611-622.
42. Papetti M, Wontakal SN, Stopka T, Skoultchi AI. GATA-1 directly regulates p21 gene expression during erythroid differentiation. *Cell Cycle*. 2010;9(10):1972-1980.
43. Libani IV, Guy EC, Melchiori L, et al. Decreased differentiation of erythroid cells exacerbates ineffective erythropoiesis in beta-thalassemia. *Blood*. 2008;112(3):875-885.
44. Yang B, Kirby S, Lewis J, Detloff PJ, Maeda N, Smithies O. A mouse model for beta 0-thalassemia. *Proc Natl Acad Sci U S A*. 1995;92(25):11608-11612.
45. Ciavatta DJ, Ryan TM, Farmer SC, Townes TM. Mouse model of human beta zero thalassemia: targeted deletion of the mouse beta maj- and beta min-globin genes in embryonic stem cells. *Proc Natl Acad Sci U S A*. 1995;92(20):9259-9263.
46. Chen K, Liu J, Heck S, Chasis JA, An X, Mohandas N. Resolving the distinct stages in erythroid differentiation based on dynamic changes in membrane protein expression during erythropoiesis. *Proc Natl Acad Sci U S A*. 2009;106(41):17413-17418.
47. de Jong MO, Westerman Y, Wagemaker G, Wognum AW. Coexpression of Kit and the receptors for erythropoietin, interleukin 6 and GM-CSF on hemopoietic cells. *Stem Cells*. 1997;15(4):275-285.
48. Terszowski G, Waskow C, Conradt P, et al. Prospective isolation and global gene expression analysis of the erythrocyte colony-forming unit (CFU-E). *Blood*. 2005;105(5):1937-1945.
49. Yalcin S, Marinkovic D, Mungamuri SK, et al. ROS-mediated amplification of AKT/mTOR signalling pathway leads to myeloproliferative syndrome in Foxo3(-/-) mice. *EMBO J*. 2010;29(24):4118-4131.
50. Zhang Y, Paikari A, Sumazin P, et al. Metformin induces FOXO3-dependent fetal hemoglobin production in human primary erythroid cells. *Blood*. 2018;132(3):321-333.
51. You H, Pellegrini M, Tsuchihara K, et al. FOXO3a-dependent regulation of Puma in response to cytokine/growth factor withdrawal. *J Exp Med*. 2006;203(7):1657-1663.
52. Villunger A, Michalak EM, Coultas L, et al. p53- and drug-induced apoptotic responses mediated by BH3-only proteins puma and noxa. *Science*. 2003;302(5647):1036-1038.
53. Abbas T, Dutta A. p21 in cancer: intricate networks and multiple activities. *Nat Rev Cancer*. 2009;9(6):400-414.
54. An JH, Jang SM, Kim JW, Kim CH, Song PI, Choi KH. The expression of p21 is upregulated by Forkhead box A1/2 in p53-null H1299 cells. *FEBS Lett*. 2014;588(21):4065-4070.
55. Tinkum KL, White LS, Marpegan L, Herzog E, Piwnica-Worms D, Piwnica-Worms H. Forkhead box O1 (FOXO1) protein, but not p53, contributes to robust induction of p21 expression in fasted mice. *J Biol Chem*. 2013;288(39):27999-28008.
56. Price JG, Idoyaga J, Salmon H, et al. CDKN1A regulates Langerhans cell survival and promotes Treg cell generation upon exposure to ionizing irradiation. *Nat Immunol*. 2015;16(10):1060-1068.
57. Traxler EA, Thom CS, Yao Y, Paralkar V, Weiss MJ. Nonspecific inhibition of erythropoiesis by short hairpin RNAs. *Blood*. 2018;131(24):2733-2736.
58. Ferber EC, Peck B, Delpuech O, Bell GP, East P, Schulze A. FOXO3a regulates reactive oxygen metabolism by inhibiting mitochondrial gene expression. *Cell Death Differ*. 2012;19(6):968-979.
59. Rimmele P, Liang R, Bigarella CL, et al. Mitochondrial metabolism in hematopoietic stem cells requires functional FOXO3. *EMBO Rep*. 2015;16(9):1164-1176.
60. Peserico A, Chiacchiera F, Grossi V, et al. A novel AMPK-dependent FoxO3A-SIRT3 intramitochondrial complex sensing glucose levels. *Cell Mol Life Sci*. 2013;70(11):2015-2029.

61. Kops GJ, Medema RH, Glassford J, et al. Control of cell cycle exit and entry by protein kinase B-regulated Forkhead transcription factors. *Mol Cell Biol*. 2002;22(7):2025-2036.
62. Essers MA, Weijzen S, de Vries-Smits AM, et al. FOXO transcription factor activation by oxidative stress mediated by the small GTPase Ral and JNK. *EMBO J*. 2004;23(24):4802-4812.
63. Zhan M, Brooks C, Liu F, Sun L, Dong Z. Mitochondrial dynamics: regulatory mechanisms and emerging role in renal pathophysiology. *Kidney Int*. 2013;83(4):568-581.
64. Arnoult D, Soares F, Tattoli I, Girardin SE. Mitochondria in innate immunity. *EMBO Rep*. 2011;12(9):901-910.
65. Ma K, Chen G, Li W, Kepp O, Zhu Y, Chen Q. Mitophagy, mitochondrial homeostasis, and cell fate. *Front Cell Dev Biol*. 2020;8:467.
66. Deng C, Zhang P, Harper JW, Elledge SJ, Leder P. Mice lacking p21CIP1/WAF1 undergo normal development, but are defective in G1 checkpoint control. *Cell*. 1995;82(4):675-684.
67. Brugarolas J, Chandrasekaran C, Gordon JI, Beach D, Jacks T, Hannon GJ. Radiation-induced cell cycle arrest compromised by p21 deficiency. *Nature*. 1995;377(6549):552-557.
68. Eijkelenboom A, Burgering BM. FOXOs: signalling integrators for homeostasis maintenance. *Nat Rev Mol Cell Biol*. 2013;14(2):83-97.
69. Menon V, Ghaffari S. Transcription factors FOXO in the regulation of homeostatic hematopoiesis. *Curr Opin Hematol*. 2018;25(4):290-298.
70. Vousden KH, Lane DP. p53 in health and disease. *Nat Rev Mol Cell Biol*. 2007;8(4):275-283.
71. Chen J. The cell-cycle arrest and apoptotic functions of p53 in tumor initiation and progression. *Cold Spring Harb Perspect Med*. 2016;6(3):a026104.
72. Ghanem L, Steinman R. A proapoptotic function of p21 in differentiating granulocytes. *Leuk Res*. 2005;29(11):1315-1323.
73. Kang KH, Kim WH, Choi KH. p21 promotes ceramide-induced apoptosis and antagonizes the antideath effect of Bcl-2 in human hepatocarcinoma cells. *Exp Cell Res*. 1999;253(2):403-412.
74. Hingorani R, Bi B, Dao T, Bae Y, Matsuzawa A, Crispe IN. CD95/Fas signaling in T lymphocytes induces the cell cycle control protein p21cip-1/WAF-1, which promotes apoptosis. *J Immunol*. 2000;164(8):4032-4036.
75. Lavin Y, Winter D, Blecher-Gonen R, et al. Tissue-resident macrophage enhancer landscapes are shaped by the local microenvironment. *Cell*. 2014;159(6):1312-1326.
76. Myneni VD, Szalayova I, Mezey E. Differences in steady-state erythropoiesis in different mouse bones and postnatal spleen. *Front Cell Dev Biol*. 2021;9:646646.
77. Chow A, Huggins M, Ahmed J, et al. CD169(+) macrophages provide a niche promoting erythropoiesis under homeostasis and stress. *Nat Med*. 2013;19(4):429-436.
78. Ramos P, Casu C, Gardenghi S, et al. Macrophages support pathological erythropoiesis in polycythemia vera and beta-thalassemia. *Nat Med*. 2013;19(4):437-445.
79. Hu J, Liu J, Xue F, et al. Isolation and functional characterization of human erythroblasts at distinct stages: implications for understanding of normal and disordered erythropoiesis in vivo. *Blood*. 2013;121(16):3246-3253.